

CONTROL ALGORITHMS FOR SYSTEM INTEGRATION OF HEAT PUMPS: STEADY STATE AND SEASONAL ANALYSIS

*D. Finn, F. Murphy and S. Shannon
School of Electronic, Electrical and Mechanical Engineering,
University College Dublin, Ireland.*

Abstract: This paper is concerned with the development of control strategies aimed at real-time optimisation and system integration of heat pumps in building heating and cooling applications. The research was motivated by the requirement to develop and implement control algorithms for a reversible water-to-water ground source heat pump. This was achieved by considering a secondary side control strategy, which examined the influence of secondary fluid flow rates on both the heat pump and the integrated system performance. Two control schemes were identified: (i) a *Performance Maximisation* approach, which was achieved by adjusting the secondary fluid flow rates to settings that maximised COP performance of the overall heat pump system, and (ii) a *Capacity Maximisation* approach where the secondary fluid flow rates were set to their maximum settings, thus maximising the heating or cooling capacity of the heat pump. A steady state model of the heat pump subject to different water inlet boundary conditions, facilitated the development of performance maps, thereby allowing the variation in heat pump capacity and compressor power consumption with secondary fluid flow conditions to be examined. Further development of the system model, to include the ground and building system loops was undertaken, thereby allowing overall system performance to be examined. Steady state and seasonal performance simulations of the integrated heat pump, ground loop and building were analysed. The two control schemes are compared in terms of their steady state and seasonal performances and the modelled predictions are compared with experimental data collected from a ground source heat pump installation.

Key Words: Heat Pump, Control Algorithm, Optimisation

1 INTRODUCTION

Optimisation of heat pump systems through implementation of sophisticated control strategies has the potential to improve heat pump system performance thereby reducing overall power consumption, improving heat pump COP and ultimately decreasing CO₂ emissions. The control algorithms that are currently utilised in typical heat pump installations focus primarily on on-off capacity control by means of compressor cycling in conjunction with a thermostatic expansion valve to optimise evaporator performance (Karlsson and Fahlen 2003). Although these forms of control are widely deployed, they may not in certain applications be necessarily the most efficient, versatile or effective. Furthermore, opportunities exist for the application of control beyond the immediate vapour compression cycle. Various studies have shown that in certain cases energy savings can be achieved by employing variable speed compressors (Pareira and Parise 1993, Vargas and Parise 1994, Qureshi and Tassou 1995). The use of a variable speed compressor normally requires the inclusion of an electronic expansion valve (EEV), as thermostatic expansion valves (TXV) are generally less capable of operating over the required range of flow rates. Research carried out by Aprea and Mastrullo (2002), Ding and Fu (2004) and Choi and Kim (2004) suggests that EEVs may outperform TXVs in heat pumps under certain operating conditions.

EEVs are generally more flexible, offer more accurate control and achieve superior system efficiencies compared to TXVs. However, they may not be suitable for all applications as they are relatively expensive, when compared with conventional expansion devices such as TXVs or capillary tubes.

The current research was motivated by the requirement to consider the feasibility of alternative control possibilities, as well as extending the influence of the control scheme beyond the heat pump vapour compression system. Additional control solutions may be exploited by considering the total heat pump system (ground source heat exchangers, building characteristics and secondary circuits) rather than the vapour compression system exclusively. Indoor and outdoor secondary circuits facilitate the movement of secondary fluids to and from the heat pump. Additional control opportunities arise for ground source heat pumps as a result of these secondary circuits. The secondary pump associated with each secondary circuit can be considered as an additional controllable component, where temperature and flowrate are controllable parameters. Furthermore, heating or cooling may be delivered by fan coils within a space, thereby providing the opportunity of further control possibilities through modulation of the fan coil and the associated space variables.

2 METHODOLOGY

Considering a standard vapour compression cycle, changes in heat exchanger saturation pressure and temperature occur when the flow rate or inlet temperature of the secondary fluid alters. In this context, the secondary fluid flow rates can be viewed as independent variables, whose values can be determined by adjusting the speeds of the circulating pumps. The secondary fluid heat evaporator and condenser inlet temperatures can then be considered as dependent variables, whose magnitudes are a function of the secondary fluid flow rates, the heat pump performance and the building behaviour. Increasing the secondary fluid flow rate increases the overall heat exchanger U-value due to increased fluid-side convection. Therefore for an evaporator, increases in the secondary flow rate results in an increased outlet temperature and a higher mean secondary fluid temperature. This in turn raises the evaporator saturation pressure. The greater U-value also effects a reduced mean heat exchanger ΔT , which also increases evaporator saturation pressure. Similarly, raising the flow rate of water in the condenser causes a lower outlet temperature, a lower mean heat exchanger ΔT and a lower average secondary fluid temperature. This results in a reduced condenser pressure. Therefore increasing the water flow rate in either the evaporator or the condenser reduces the differential between the high and low side saturation pressures, which in turn increases the COP of the heat pump. Both the temperature and flow rates of the secondary fluids influence heat pump capacity, compressor electrical power consumption and the parasitic power consumption associated with the secondary pumps. Using the secondary flowrates as control parameters, two control schemes can be identified as follows: performance optimisation and capacity maximisation.

Performance Maximisation is achieved by adjusting the secondary fluid flow rates to values that maximise the system COP, i.e., the ratio of the heat pump capacity to the total system power consumption (compressor, the indoor pump and the outdoor pump).

Capacity Maximisation occurs when the secondary fluid flow rates are set to their maximum values; thus maximising the heating or cooling capacity of the heat pump, but not necessarily optimising system COP.

Although increased secondary fluid flow rate results in improved heat pump performance, a system penalty is incurred. Raising the flow rate by increasing the speed of the circulation pump brings about an increase in the pump power consumption. The *performance maximisation* scheme aims to optimise system COP, by maximising the heat pump capacity,

whilst minimising the total electrical power consumption. The goal of the *capacity maximisation* scheme is to maximise the heating or cooling capacity; irrespective of the impact on system power consumption.

The concept of a system coefficient of performance (COP_{sys}) is used to quantify the benefit gained (heating / cooling delivered) relative to the total power consumption. Equations 1 and 2 illustrate the system coefficient of performance for a heat pump in cooling mode and heating mode respectively:

$$COP_{Csys} = \frac{\dot{Q}_c}{P_c + P_{pe} + P_{pc}} \quad (1)$$

$$COP_{Hsys} = \frac{\dot{Q}_H}{P_c + P_{pe} + P_{pc}} \quad (2)$$

At each operating condition, there exists unique evaporator and condenser flow rates that optimise the system COP by maximising the system capacity and minimising the total system power consumption. In this case, the goal of the control strategy was to maximise the system performance. Alternatively, the aim of the control strategy may be to maximise the heating or cooling capacity of the heat pump. To achieve capacity maximisation, it is necessary to maximise the flow rates of the secondary fluids on both sides of the heat pump. The secondary fluid flow rates are independent variables that can be adjusted by modulating the speeds of the pumps. Therefore this control scheme may be implemented by employing either multiple speed pumps or continuously variable speed pumps.

3 STEADY STATE HEAT PUMP PERFORMANCE

3.1 Heat Pump System

The laboratory prototype heat pump utilised in this work, which is shown in Figure 1, is a reversible water-to-water heat pump which uses propane as its primary refrigerant. It was installed at the Universidad Politécnica de Valencia (UPV) under the auspices of a 6FP EU supported project. The unit is a reversible water to water ground-source unit rated at 18.5kW heating (Condenser 25/30 – Evaporator 12/7) and 15kW cooling (Evaporator 25/30– Evaporator 12/7) and utilises six boreholes on the ground side in conjunction with twelve fan coil units on the building side. A schematic of the integrated system including the ground and building loops is also shown in Figure 1.

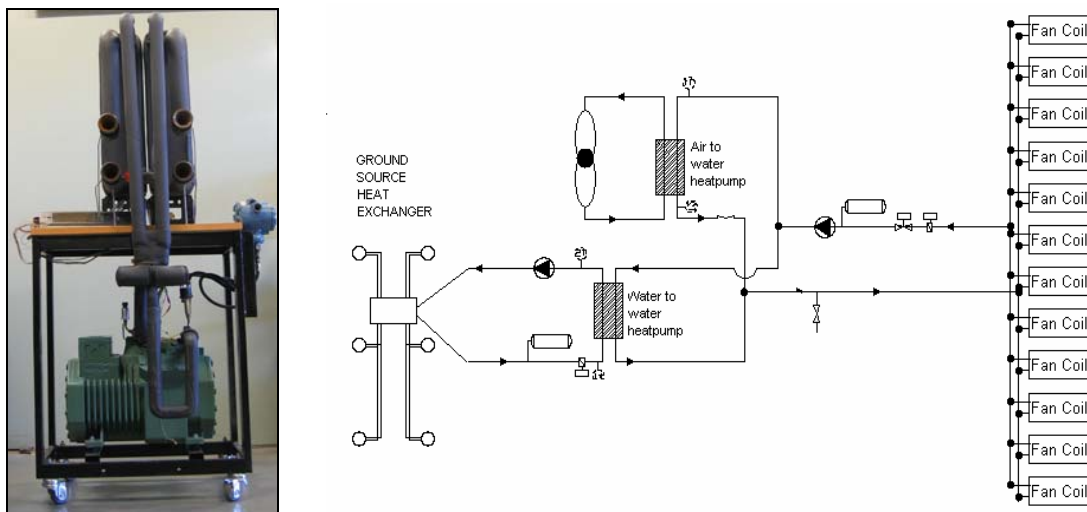


Figure 1: Heat pump laboratory prototype and building system integration

3.2 Heat Pump Performance Maps

The influence that secondary fluid flow rates had on performance was investigated by considering the variation in cooling and heating capacity as well as compressor electrical power consumption with evaporator flow rate at constant condenser flow rate; and with condenser flow rate at constant evaporator flow rate. The data collected from the heat pump installation at UPV and was analysed and correlated using the Engineering Equation Solver (EES 2008) resulting in the various performance maps shown in Figures 2 to 6.

The results presented in Figure 2 are associated with an evaporator water inlet temperature of 12°C and a condenser temperature difference of 5°C. Similar trends were also observed at other inlet temperatures as shown by Figure 3. Cooling capacity increases with increased evaporator flow rate, because of the increased evaporator saturation pressure. In addition, cooling capacity is observed to increase with increased evaporator water inlet temperature.

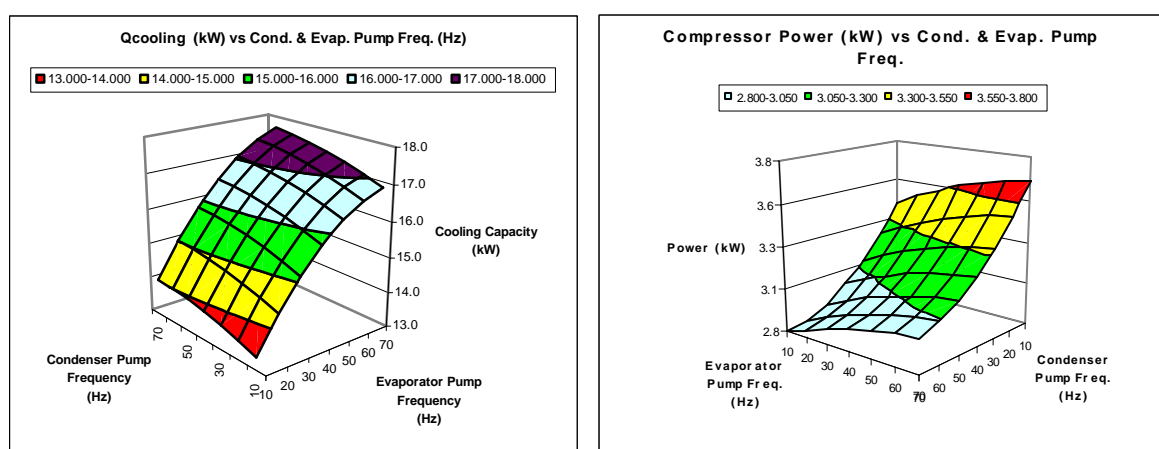


Figure 2: Variation in cooling capacity and compressor power consumption with evaporator and condenser pump speed

Figure 4 shows the heat pump COP based on compressor power consumption only. It can be seen from these results that COP increases as either evaporator or condenser pump flow rate is increased.

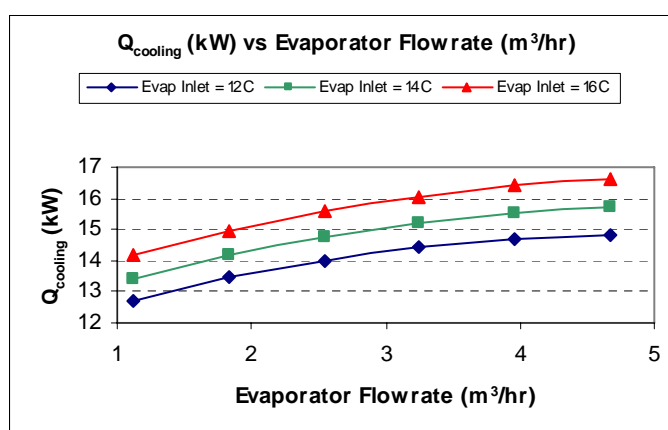


Figure 3: Variation in capacity with evaporator secondary temperature

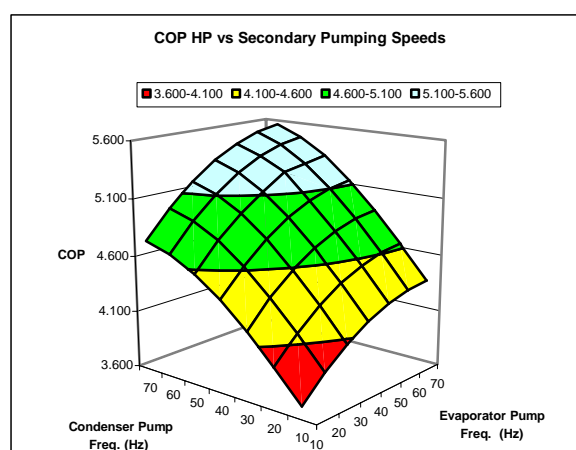


Figure 4: Variation in COP (cooling) with evaporator and condenser pump speed

3.3 Steady State System Performance Optimisation

In order to evaluate overall system performance, the performance maps outlined in Figures 2 to 4 were correlated and incorporated along with the secondary pump performance characteristics into a system model that includes the ground and building loops as outlined in Figure 1. This was achieved by determining correlation curves for the building and ground loops and integrating them within a single system model (EES 2008).

Figure 5 shows the total power consumption of the heat pump and secondary pumps as the speed of the secondary pumps are varied. It is noted that maximum power is consumed when both pumps are operating at their upper speeds of 70Hz. In addition, an increase in power consumption is also evident at lower pump speeds and this can be attributed to additional compressor power requirements due to the increased pressure lift.

Considering the overall system COP, which is based on heat pump and secondary pumps as defined by Equations 1 and 2, a dome shaped performance map is observed in Figure 6. Closer examination of Figure 6 shows that a peak COP can be identified, which for cooling occurs when the internal circulation pump operates at a frequency of 30Hz and the external circulation pump operates at 40Hz. Similar trends were evident for the system operating under heating mode.

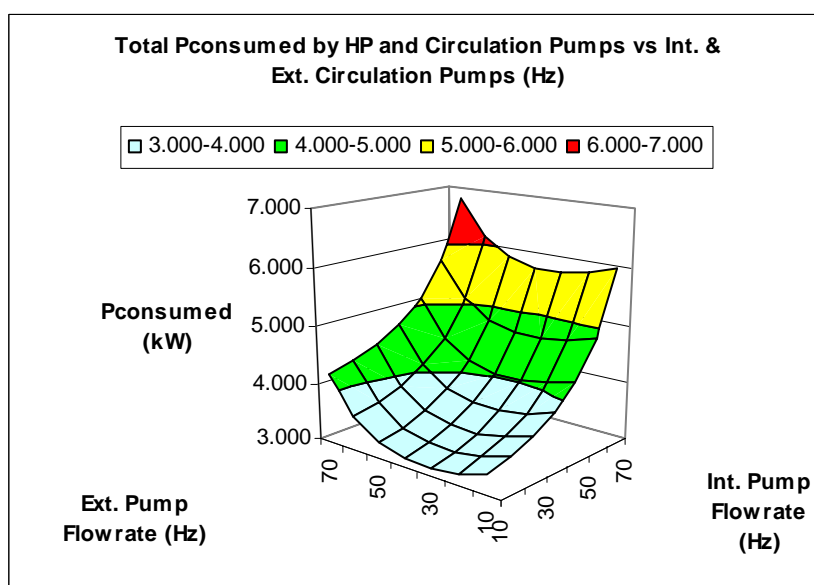


Figure 5: Total heat pump power consumption vs secondary pump speeds

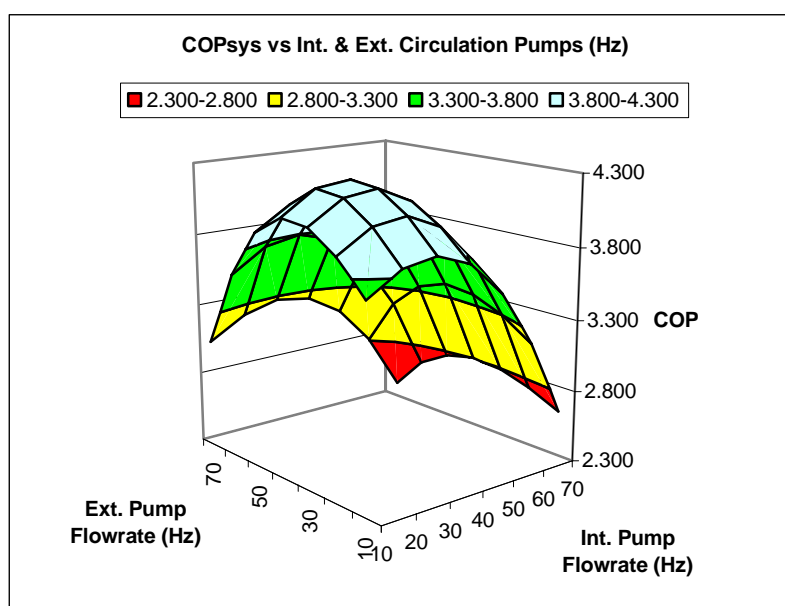


Figure 6: Overall heat pump COP vs secondary circulation pumps speeds

A comparison was carried out of the steady state performances of the *performance maximisation* and the *capacity maximisation* operating schemes. Table 1 summarises the overall system COP associated with both operating schemes with all other parameters maintained constant except for the flow rates of the circulation pumps. It can be observed that the *performance maximisation* scheme results in a better system COP without suffering a significant penalty in cooling capacity. The capacity maximisation provides additional capacity but has a reduced system COP

In both heating and cooling modes, the COP of the heat pump alone was higher in the *capacity maximisation* mode; whereas the system COP was higher in the *performance maximisation* mode.

	Performance Maximisation	Capacity Maximisation	Default Operation
	Evaporator 30Hz Condenser 40Hz	Evaporator 70Hz Condenser 70Hz	Evaporator 50Hz Condenser 50Hz
HP Power Consumption (kW)	3.01	2.93	2.99
System Power Consumption (kW)	3.40	6.78	4.16
$Q_{cooling\ HP}$ (kW)	14.46	16.28	15.64
COP HP	4.80	5.56	5.26
COP System	4.25	2.40	3.76

Table 1: Capacity maximisation and performance optimisation results in cooling mode.

4 SEASONAL HEAT PUMP PERFORMANCE

The seasonal performance of a heat pump system is dependent on the annual heating and cooling demand of the building. The dynamic operation of the heat pump, which reflects the transient behaviour of the building, was approximated using a quasi-steady state approach based on an interval analysis based on one hour. The average heat pump capacity over this period was determined by calculating the average rate of building heat loss or heat gain for this period.

For the seasonal analysis, the heat pump system was used to condition twelve spaces within the Applied Thermodynamics Department Building at UPV. The U-value and total area of the exterior walls was $1.198 \text{ W/m}^2 \text{ K}$ and 126.6 m^2 respectively, thus yielding a building UA value of 151.65 W/K . The U-value of the interior walls was $2.059 \text{ W/m}^2 \text{ K}$. The total flow rate of ambient air into the building for ventilation and due to infiltration was $396 \text{ m}^3/\text{hr}$. Hourly ambient air temperatures for Valencia were obtained using ASHRAE data, thus facilitating the calculation of the rate of sensible heat loss or heat gain [ASHRAE 2005]. Transient effects, due to building thermal mass were ignored.

The following heat gains and heat losses were considered:

- Sensible heat gains and losses due the temperature difference between the conditioned space and the external ambient condition.
- Infiltration air losses and gains.
- Heat gains and losses due to ventilation air requirements.
- Fixed heat gains from people, lighting and equipment.
- Fixed heat losses and gains due to heat transfer to or from adjacent rooms.

The heat gains and losses were calculated on an hourly basis, and were used to generate a quasi-steady state approximation of the heat pump capacity over the duration of a year. The year was split into a heating season from November to February and a cooling season from March to October.

The total annual heating and cooling loads were $15,714 \text{ kWh}$ (79 kWh/m^2) and $38,628 \text{ kWh}$ (193 kWh/m^2) respectively. These values compared favourably with other data obtained from the literature. Eichhammer and Schlomann (2000) calculated typical annual building heating demands in Spain of 77.9 kWh/m^2 , whilst an EU supported project reported an average annual building cooling loads in Vilanova, Spain of 172.8 kWh/m^2 (ECG 2008). A maximum steady space heating requirement of 7.12 kW (35.6 W/m^2) occurred in January; and a maximum space cooling requirement of 10.49 kW (52.5 W/m^2) occurred in August. The capacity of the heat pump was therefore adequate to meet the maximum heating and cooling requirements.

4.1 Quantification of Cycling Losses

Capacity modulation was achieved using compressor on-off cycling. When analysing the transient behaviour of the heat pump system, it was necessary to quantify the cycling losses that occurred. Compressor cycling introduces inefficiencies for the following reasons (Tassou and Voitsis 1992; Henderson, Parker and Huang, 2000):

- Transient losses associated with the thermal mass of the compressor, other heat pump components and secondary system components.
- Transient losses due to refrigerant migration from the high pressure side to the low pressure side during the off-cycle.
- Off-cycle or standby power consumption (due to off-cycle pump power consumption, crankcase heaters and controls).

The part load performance of a heat pump is dependent on the following parameters:

- Time constant associated with the response of the system at startup.
- Cycling rate of the heat pump.

Parken, Beausoliel and Kelly (1977) combined these effects in a degradation coefficient (C_d), which was used to develop a part load correlation. In their approach, they used laboratory and field test data to ascertain the value of C_d . The Part Load Function (PLF) could then be determined at any defined Part Load Ratio (PLR), using Equations 3 and 4. Knowledge of the steady state efficiency and the PLF then allowed the part load efficiency to be calculated using Equation 5.

$$PLF = 1 - C_d(1 - PLR) \quad (3)$$

$$PLR = \frac{\text{Load}}{\text{Capacity}} \quad 0 \leq PLR \leq 1 \quad (4)$$

$$PLF = \frac{\text{Part Load Efficiency}}{\text{Steady State Efficiency}} \quad 0 \leq PLF \leq 1 \quad (5)$$

An approximation for the degradation coefficient (C_d) may be found using Equation 6, which was developed Henderson and Rengarajan (1996). This value of C_d may then be used in Eqn 3 to estimate the PLF curve using the linear C_d method.

$$C_d = 4 \tau N_{\max} \left[1 - e^{-1/(4 \tau N_{\max})} \right] \quad (6)$$

These correlations were developed for systems operating in the cooling mode. Bonne et al. (1980) showed that the transient behaviour of heat pumps is similar in both the heating and cooling modes. Parken et al. (1977) showed that the heating and cooling part load curves of residential heat pumps are approximately identical. Therefore the same correlations are applied in both modes. Using the Linear C_d method, proposed by Parken et al. (1977), the part load COP (COP_{pl}) was found using Equation 7.

$$COP_{pl} = PLF \times COP_{ss} \quad (7)$$

where COP_{pl} is the COP at part load and COP_{ss} is the steady state COP.

Henderson, Huang and Parker (2000) found that seasonal energy efficiency ratio tests indicated measured values of C_d between 0.1 and 0.2. Mei (1983) also found that typical values of C_d ranged between 0.13 and 0.19. Mei (1983) also determined that the value of C_d is independent of evaporator and condenser secondary fluid temperatures. A C_d value of 0.1, which is equivalent to $N_{\max} = 2.5$ cycles per hour and $\tau = 30$ s was chosen because it reflects the part load behaviour of a *good* system, which is representative of the system used in this work. This selection was made on the basis of the definition of a *good* system, as outlined by Henderson, Huang and Parker (2000).

4.2 Seasonal Performance COP Penalty Factor

Ehrbar et al. (2003) found that the compressor electrical power consumption is approximately equal during start-up and steady state operation. Therefore the difference in COP associated with a change in PLR manifests itself as an associated change in output capacity, rather than a change in power consumption. The part load ratio was determined for each sixty minute time-step. The heat pump COP was determined at each interval, using the steady state COP values and the PLF. This revised capacity indicated the fraction of the sixty minute interval that the heat pump was required to run in order to meet the heating or cooling demand for that period. The heat pump rate of electrical power consumption was known from the steady state simulations. The power consumption of the secondary pumps was also known from the

steady state investigation. Therefore integrating the total steady state power consumption figure over the duration of the run-time provided the total electrical power consumption for that period. This process was carried out for every one-hour interval. The annual power consumption was then determined by integrating the power consumption at each interval over the year.

For the performance maximisation operation mode, a seasonal penalty of 0.935 was found to apply to system COP for the heating season (November-February), whereas a penalty of 0.829 applied to the cooling season performance COP (March-October). For the capacity maximisation mode, COP penalty factors of 0.94 and 0.843 applied to the heating and cooling seasonal analysis, respectively. This resulted in an 11% reduction in annual power consumption by switching from capacity maximisation to performance maximisation routines. The overall finding was that the performance maximisation routine consumed less electricity than the capacity maximisation routine, whilst delivering the same total quantity of heating and cooling over the duration of the year.

5 CONCLUSIONS

Heat pump secondary side control is the focus of this work. Optimisation can be achieved either by (i) maximisation of the system COP or (ii) maximisation of capacity. System COP maximisation is achieved by increasing the heat pump COP, without raising the electrical power consumption of the secondary pumps excessively. Alternatively, capacity maximisation may be achieved by setting the flow rate of the secondary fluids to their highest levels. The secondary fluid flow rates that bring about the desired operation may be set using variable speed pumps.

In heating mode, switching from capacity maximisation to performance maximisation brought about a 12% increase in system COP, with an associated 5% reduction in capacity. In cooling mode, switching from capacity maximisation to performance optimisation yielded a 14 % increase in system COP, with an associated 3% reduction in capacity.

The key conclusion of the seasonal performance evaluation was that the system performance optimisation technique yielded an 11% reduction in total annual electrical energy consumption relative to the capacity maximisation technique.

A holistic control strategy optimises the heat pump performance in response to a number of parameters, thus requiring a multiple input multiple output approach. A comprehensive holistic control strategy would rely on real-time knowledge of the building heating or cooling loads; the transient heat pump, ground source heat exchanger and air conditioning system performances; real-time weather data and real-time electricity tariffs. A number of parameters would then be used in an optimisation routine, which dictates the appropriate operating conditions and output variables in real time. In a multiple output scenario there is potential to simultaneously control the compressor capacity (through use of a variable speed drive), the flow rates of the secondary fluids and the air flow rates of the fan coil units.

NOMENCLATURE

C_d	=	Degradation co-efficient
COP_{pl}	=	Part load co-efficient of performance
COP_{ss}	=	Steady-state co-efficient of performance
$COP_{c_{sys}}$	=	System coefficient of performance for cooling mode
$COP_{h_{sys}}$	=	System coefficient of performance for heating mode
\dot{Q}_c	=	Cooling capacity (kW)
\dot{Q}_h	=	Heating capacity (kW)
P_c	=	Compressor power consumption (kW)
P_{pc}	=	Condenser pump power consumption (kW)
P_{pe}	=	Evaporator pump power consumption (kW)
PLF	=	Part load function

ACKNOWLEDGEMENTS

This work was financially supported under the auspices of the EU FP 6 programme (Contract No. 500229-2-SHERHPA). The authors gratefully acknowledge the availability of experimental data provided by the Applied Thermodynamics Group of the Universidad Politécnica de Valencia, Spain.

REFERENCES

- ASHRAE Fundamentals Handbook – SI Edition 2005, Atlanta : American Society of Heating, Refrigerating and Air-Conditioning Engineers. ISBN 4046368400.
- Aprea, C & Mastrullo, R 2002, 'Experimental Evaluation of Electronic and Thermostatic Expansion Valves Performances using R22 And R407C', *Applied Thermal Engineering*, vol. 22, no. 2, pp. 205–218.
- Bonne, U., Patani, A., Jacobson, R.D. and Mueller, D.A. 1980, "Electric Driven Heat Pump Systems: Simulations and Controls II", *ASHRAE Transactions*, vol. 86, part 1, pp. 697-705.
- Choi, J & Kim, Y 2004, 'Influence of The Expansion Device on the Performance of a Heat Pump using R407C under a Range of Charging Conditions', *Int. Journal of Refrigeration*, vol. 27, no.4, pp.378-384.
- Ding, G & Fu, L 2005, 'Performance Analysis and Improvement of Air-To-Water Chiller for Application in Wide Ambient Temperature Range'. *Applied Thermal Engineering*, vol. 25, no. 1, pp 135 – 145.
- EES (2008) Engineering Equation Solver. F-Chart Software. www.fchart.com (2008)
- EGC 2008 EGC Final Technical Report - Operations and Results 2001, European Green Cities, Global Renewable Energy and Environmentally Responsible Neighbourhoods and Cities Project, Reference No. BU-1001-96. Available www.europengreencities.com [Accessed March 2008].
- Eichhammer, W, Schlomann, B, 2000 'MURE Database Case Study: A Comparison of Thermal Building Regulations in the European Union', *Karlsruhe: Fraunhofer ISI*, 2000, 15 S., EUR 5-(ISI-B-94-00).

Ehrbar, M, Gubser, B, Hubacher, B, Esfandiar, S, Wirth, L, Zogg, D 2003, 'On Part-Load-Behaviour of On/Off-Controlled Heat Pumps', Proceedings of The 21st IIR Int. Congress of Refrigeration, Washington DC, US, ICR0116.

Henderson, H. and K. Rengarajan. 1996. A Model to Predict the Latent Capacity of Air Conditioners and Heat Pumps at Part Load Conditions with the Constant Fan Mode. ASHRAE Transactions. 102 (1).

Henderson, HI Jr., Parker, D, Huang, Y.J. 2000, 'Improved DOE-2's RESYS Routine: User Defined Functions To Provide More Accurate Part Load Energy Use And Humidity Predictions', Proceedings of The ACEEE Summer Study on Energy Efficiency in Buildings, Pacific Grove, CA, US, DOE-2 Report LBNL-46304.

Karlsson, F & Fahlén, P 2003, 'Energy Saving Potential of Capacity Controlled Brine-To-Water Heat Pumps, Proceedings of the 21st IIR International Congress of Refrigeration, Washington DC, US, ICR0262.

Parken, W.H., Beausoliel, R.W. and Kelly, G.E. 1977, "Factors Affecting the Performance of a Residential Air-to-Air Heat Pump", *ASHRAE Transactions*, vol. 83, part 1, pp. 839-849.

Parise, JAR 1985, 'Heat Pumps: A Survey on Heat Sources', Proceedings of the 8th Brazillian Congress of Mechanical Engineers, Sao Jose dos Campos, Brazil. Cited in: Parreira, EP & Parise, JAR 1993, 'Performance Analysis Of Capacity Controlled Devices For Heat Pump Reciprocating Compressors', *Heat Recovery Systems and CHP*, vol. 13, no. 5, pp. 451-461.

Parreira, EP & Parise, JAR 1993, 'Performance Analysis of Capacity Controlled Devices for Heat Pump Reciprocating Compressors', *Heat Recovery Systems and CHP*, vol. 13, no. 5, pp. 451-461.

Qureshi, TQ & Tassou. SA 1995, 'Variable Speed Capacity Control in Refrigeration Systems', *Applied Thermal Engineering*, vol. 16, no. 2, pp. 103-113.

Riviere, P, Flach-Malaspina, N & Lebreton, J 2004, 'A New Installation for Part Load Testing of Air to Water Single Stage Chillers and Heat Pumps', Proceedings of the 10th International Refrigeration and Air Conditioning Conference, Purdue, US, R086.

Tassou, S.A. & Votsis P. 1992, 'Transient Response and Cycling Losses of Air-To-Water Heat Pump Systems', *Heat Recovery Systems and CHP*, vol. 12, no. 2, pp. 123-129.

Vargas, JVC & Parise, JAR 1995, 'Simulation in Transient Regime of a Heat Pump with Closed-Loop On-Off Control', *Int. Journal of Refrigeration*, vol. 18, no. 4, pp. 235-243.